

EXPERIMENTAL SECTION

Materials. Oligonucleotides designed in this study were synthesized by Beijing Dingguo Biotechnol. Co. Ltd. (Beijing, China), which were purified by HPLC and confirmed by mass spectrometry. The sequence of the aptamers is 5'-ACCTG GGGGA GTATT GCGGA GGAAG GT-3'. DNA stock solution was obtained by dissolving oligonucleotides in tris-HCl buffer solutions (pH 7.4). Each oligonucleotide was heated to 90 °C for 5 min, and slowly cooled down to room temperature (RT) before usage. Adenosine-5'-triphosphate (ATP) standards and DNase I (Recombinant DNase I: 1000 U mL⁻¹) were purchased from Dingguo Biotechnol. Co. Ltd. (Beijing, China). Poly(vinylpyrrolidone) (PVP, K-30), *o*-phenylenediamine (OPD) and HAuCl₄·4H₂O were purchased from Sinopharm Chem. Re. Co. Ltd. (Shanghai, China). All reagents were of analytical grade and used as received without further purification. Ultrapure water obtained from a Millipore water purification system (≥18 MΩ, Milli-Q, Millipore) was used in all runs. Phosphate-buffered saline (PBS, 0.01 M, pH 7.4) solution was prepared by adding 1.221 g K₂HPO₄, 0.1362 g KH₂PO₄, and 0.7455 g KCl into 1000 mL ultrapure water.

Preparation of Au(III)-Assisted Core-Shell Iron Oxide@Poly(*o*-phenylenediamine) Nanostructures (MB@Au-POPD). Prior to experiment, nano-Fe₃O₄ particles (cores) (50 nm in diameter) were prepared by co-precipitation of Fe^(II) and Fe^(III) chlorides (Fe^{II}/Fe^{III} ratio of 0.5) in alkaline solution as described in the literatures.¹ Synthesis of the MB@Au-POPDs was as follows according to the literatures with some modification² by using one-pot *in situ* polymerization method: 500 mg of Fe₃O₄ nanoparticles were initially added into 20 mL NaCl solution (0.5 M)

containing 0.025 M sodium dodecyl sulphate (SDS), and stirred for 4 h. After washing with water, the SDS-Fe₃O₄ composites were redispersed into 10 mL poly(vinyl pyrrolidone) (PVP) aqueous solution (1%, w/w), and the mixture was vigorously stirred for another 2 h at RT to obtain PVP-coated Fe₃O₄ nanoparticles. Excess SDS and PVP were removed in the supernatant fraction after centrifugation. Following that, the obtained precipitate was re-dispersed into 3 mL HAuCl₄ (1%, w/w) aqueous solution, and shaken slightly for 1 h at RT to make the [AuCl₄]⁻ ions assemble on the PVP-functionalized Fe₃O₄. Subsequently, 0.07 g *o*-phenylenediamine was injected into the mixture, and stirred for 1 h at RT (i.e. W_[HAuCl₄] : W_[OPD] ≈ 3 : 7). During this process, the Au(III) was reduced to zero-valent Au⁰, and the OPD was polymerized onto the surface of magnetic beads to form a layer of poly(OPD) composite membrane. Finally, the obtained MB@Au-POPd nanostructures were collected by centrifugation, and stored at 4 °C for further use.

Electrochemical Measurement. All electrochemical measurements were carried out on a CHI 630D Electrochemical Analyzer (Shanghai, China) with a gold disk (2 mm in diameter) working electrode, a platinum wire auxiliary electrode and a saturated SCE reference electrode. The system consisted of a six-way valve equipped with a 1-mL syringe pump, and connected through a teflon tubing with the flow cell. The gold electrode was installed at the bottom of the cell, and an external permanent BaFe₁₂O₁₉ magnet with pot shape (10 mm in diameter and 5 mm in depth, 410-430 mT) was set under the working electrode. The carrier buffer (PBS, pH 7.4), MB@Au-POPd, and ATP aptamer were introduced at 500 μL min⁻¹ *via* a control valve-based

injection loop, respectively. The analyte and DNase I were directly injected into the cell by using a microsyringe.

The analytical scheme of the electrochemical aptasensors toward ATP standards was carried out as following processes: (i) 200 μL of MB@Au-POPD ($C_{[\text{MB@Au-POPD}]} \approx 10 \text{ mg mL}^{-1}$) was injected into the detection cell, and collected on the surface of gold electrode with an external magnet; (ii) 200 μL aptamer (5.0 μM) was flowed into the cell, and incubated for 32 min at RT without the magnet to form the MB@Au-POPD/aptamer complexes; (iii) 50 μL of ATP sample with various concentrations and DNase I (50 μL , 30 U mL^{-1}) were added into the cell, and incubated for 50 min without the magnet; and (iv) square wave voltammetric (SWV) measurement was performed in pH 7.4 PBS with the external magnet from -700 mV to -300 mV (*vs.* SCE) (Amplitude: 25 mV; Frequency: 15 Hz; Increase *E*: 4 mV). All incubations and measurements were carried out using stopped-flow technique at RT (25 ± 1.0 °C). After each step, the detection cell was washed by using pH 7.4 PBS in the presence of the external magnet. Analyses were always made in triplicate.

RESULTS AND DISCUSSION

Characterizations of MB@Au-POPD Nanostructures. Fig. S1a shows typical transmission electron microscope (TEM, Hitachi H-7650, Japan) of the as-prepared MB@Au-POPD nanostructures, and the mean size was about 120 nm. Compared with our previous report on bare magnetic beads,³ the functionalized nanostructures exhibited well-separated spherical particles with a relatively low polydispersity. Moreover, we also could observe a layer of craggy polymer

nanoshell coating on the nanostructure surface. Whether were magnetic beads encapsulated into the nanocomposites or whether was the OPD polymerized onto the magnetic beads, however? To monitor this issue, we used fourier transfer infrared spectrometry (FTIR, Perkin-Elmer 2000, USA) to investigate the nanocomposites. As seen from Fig. S2b, two characteristic absorption peaks at 1510 cm^{-1} and 1640 cm^{-1} corresponding to the vibration of benzene ring were obviously observed. Detailedly, the peak at 1510 cm^{-1} mainly derived from the combination of N-H bending and C-N stretching vibration. The results suggested that the OPD might be formed on the nanocomposites. Significantly, we can also observe the characteristic adsorption peaks for the Fe-O bond vibration at 627 cm^{-1} and 453 cm^{-1} , indicating the existence of Fe and O elements in the nanocomposites.⁴ But, the binary compound (M_xO_y) was Fe_2O_3 or Fe_3O_4 ? To further confirm the phase purity of magnetic beads, pure magnetic beads have also been characterized by Raman spectroscopy (XploRA, Horiba Sci.) (Fig. S1c). In the Raman spectra, although most peaks of Fe_3O_4 are close to Fe_2O_3 peaks, Fe_2O_3 exhibits much stronger peaks between 1300 cm^{-1} and 1600 cm^{-1} than observed for Fe_3O_4 . As shown in Fig. S1c, very weak peaks were in the 800 to 2000 cm^{-1} range for the sample, suggesting that the formation of Fe_2O_3 was very unlikely. Raman peaks at 322 , 468 , and 614 cm^{-1} were characteristics of Fe_3O_4 . Another important question that still remains was whether gold nanoparticles were present in the nanoshells. The as-synthesized MB@Au-POPD was characterized by XRD. As seen from Fig. S1d, except from the characteristic peaks of iron oxide (i.e. $2\theta = 30.0$, 35.0 , 43.0 , 57.0 and 63.0°), another four characteristic peaks corresponding to the elemental gold were appeared at 38 , 43 , 64 and 77° .⁵

Based on the mentioned results above, we might make a conclusion that MB@Au-POPD nanostructures were successfully synthesized *via* the proposed routine.

Optimization of Experimental Conditions. H₂AuCl₄ is a powerful oxidant and can be reduced by various reducing agents. OPD was used as a good electron donor for H₂AuCl₄.⁶ In this work, the spontaneous formation of metal Au⁰ was attributed to the direct redox to OPD and H₂AuCl₄, and the reduction of H₂AuCl₄ by OPD resulted in the formation of metal Au atoms.^{2a} The negatively charged [AuCl₄]⁻ ions were initially adsorbed on the surface of PVP-functionalized magnetic beads. Upon addition of OPD, the adsorbed [AuCl₄]⁻ ions were directly reduced to metal Au atoms, and coated on the magnetic beads. Meanwhile, the OPD molecules were transferred into the poly(OPD) polymers. Liao has discussed the formation mechanism of monodispersed colloids by aggregation of nanosize precursors and developed a kinetic model to explain the size selection in this process.^{2a} For comparison, the OPD without H₂AuCl₄ was used as the matrix entrapping the magnetic beads. However, it was observed that no poly(OPD) polymers were formed on the magnetic beads, as seen from XRD data (date not shown).

To achieve the enhancement of the electrochemical signal and stability of the MB@Au-POPD nanostructures, the effect of H₂AuCl₄/OPD ratio in the precursor mixture should be investigated. If the Au-POPD membrane was too thin, the immobilized amount of the aptamers was less, which resulted in low electrochemical signal and disadvantaged for detection of the target. Vice versus, the thick Au-POPD film might cause a relatively higher signal-to-noise ratio. As shown in Fig. S2a, the highest signal-to-background current was obtained at $W_{[H_2AuCl_4]} : W_{[OPD]} \approx 3:7$. In this

case, the evaluation was based on the shift in the current before and after the as-prepared MB@Au-POPD was incubated with excess aptamers for 32 min at RT. When the ratio was lower than 3:7, a higher current was achieved. However, the background current also increased. Thus, 3:7 of mass ratio of H₂AuCl₄ and OPD was selected for the preparation of MB@Au-POPD nanostructures.

Additionally, the assay conditions including the incubation time between MB@Au-POPD and aptamers, and MB@Au-POPD/aptamers and ATP-DNase I, should be optimized. Fig.S2b displays the incubation time between MB@Au-POPD and aptamers on the current of the aptasensors at RT. The assay was carried out based on the interaction between the aptamers and MB@Au-POPD at the absence of ATP and DNase I. As seen from Fig. S2b, the currents decreased with the increasing incubation time, and leveled off at 32 min, indicating that the interaction tended to equilibrium or saturation between MB@Au-POPD and aptamers. Therefore, 32 min was chosen for the incubation between MB@Au-POPD and aptamers.

Fig. S2c reveals the effect of incubation time of the as-prepared aptasensors with the targets on the currents. In this step, 2.0 nM ATP was used as an example. Initially, 100 μL of mixture solution containing 2.0 nM ATP and 30 U mL⁻¹ DNase I was injected into the detection cell, and incubated for various times at RT. Following that, SWV measurement was carried out in pH 7.4 PBS. As indicated from Fig. S2c, the current increased with the increase of incubation time, and reached a maximum value at 50 min. Longer incubation time did not obviously cause the change of the current. Therefore, 50 min was chosen as incubation time for the detection of ATP.

Notes and references

- 1 D. Tang, R. Yuan and Y. Chai, *J. Phys. Chem. B*, 2006, **110**, 11640.
- 2 (a) F. Liao, *Mat. Lett.*, 2005, **59**, 3132; (b) J. Noh, S. Kim, L. Lee and S. Woo, *Mat. Lett.*, 2007, **61**, 3334.
- 3 D. Tang, R. Yuan and Y. Chai, *J. Phys. Chem. B*, 2006, **110**, 11640.
- 4 J. Sun, S. Zhou, P. Hou, Y. Yang, J. Weng, X. Li and M. Li, *J. Biomed. Mat. Res. A*, 2006, Doi. 10.1002/jbm.a.30909.
- 5 D. Parajuli, H. Kawakita, K. Inoue, K. Ohto and K. Kajiyama, *Hydrometallurgy*, 2007, **87**, 133.
- 6 X. Sun, S. Dong and E. Wang, *Chem. Commun.*, 2004, **1182**.

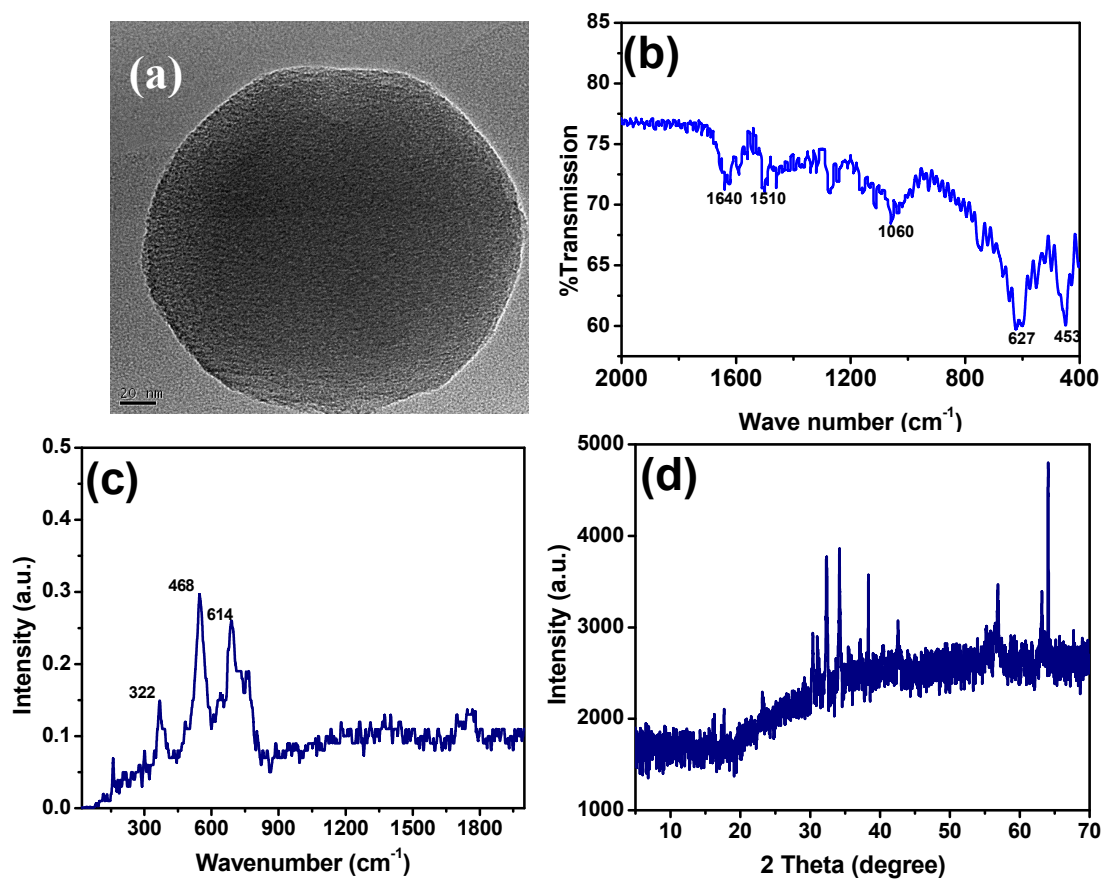


Fig. S1 (a) TEM image, (b) FTIR spectra, (c) Raman spectra (*Note*: without Au-POPD) and (d) XRD of the synthesized MB@Au-POPD nanostructures.

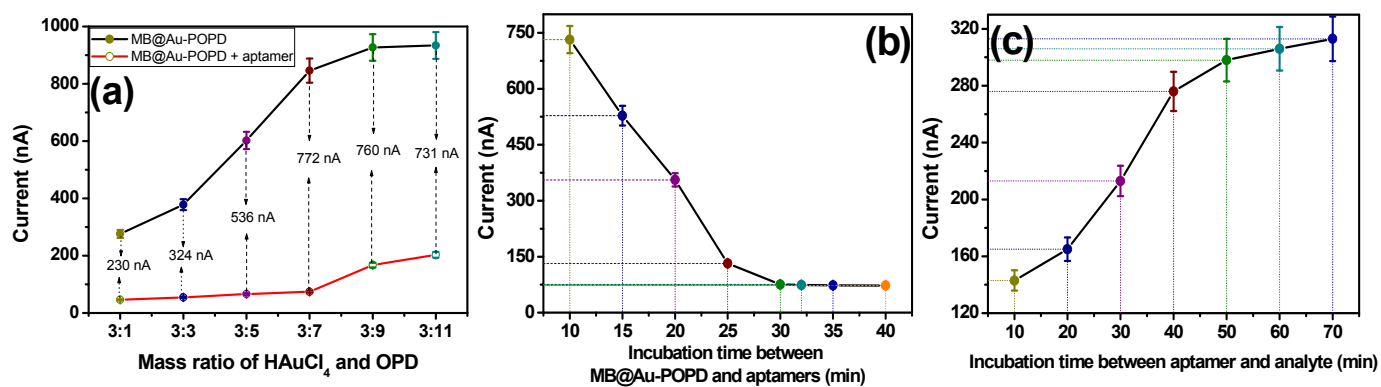


Fig. S2 Effect of (a) mass ratio of HAuCl₄ and OPD, (b) incubation time between MB@Au-OPD and aptamers, and (c) incubation time between aptamer and target ATP on the current of the aptasensors.